7th European Workshop on Structural Health Monitoring
July 8-11, 2014. La Cité, Nantes, France

EXPERIMENTAL INVESTIGATION OF FATIGUE DAMAGE IN COMPOSITE STRUCTURES CONSIDERING SECOND HARMONIC LAMB WAVES

Natalie Rauter[1], **Rolf Lammering**[1]

[1] *Insitute of Mechanics, Helmut-Schmidt-University / University of the Federal Armed Forces, 22043 Hamburg, Germany*

natalie.rauter@hsu-hh.de

ABSTRACT

To detect microstructural damages like fiber / matrix cracks and delaminations in composite materials accurately new methods are developed. Previous works have investigated and shown that the acoustical nonlinearity parameter is an appropriate tool to detect micro-structural damages like plasticity and fatigue in metal as well as thermal fatigue and impact damages in composites. In this work the second harmonic generation is used to analyze unidirectional composite specimens for fatigue damage caused by cyclic tensile load. Therefore, Lamb waves are launched and detected by piezoelectric actuator and sensor, respectively, at a certain frequency to generate cumulative second harmonic modes. The excitation frequency has to meet special conditions. The signal processing is done by using the wavelet transform. The correlation of the results of the nonlinear wave propagation to the damage state is investigated. It is shown that the relative acoustical nonlinearity parameter is sensitive to the damage state.

KEYWORDS : *Lamb waves, fatigue damage, second harmonic generation*

1. INTRODUCTION

Because of the importance to detect even microstructural damages accurately in composite material new inspections methods are developed. A promising tool is the nonlinear propagation of Lamb waves in thin-walled structures. The nonlinear wave propagation is based on the generation of higher harmonic modes due to material defects. Therefore, the existence of higher harmonic modes is an indicator for damages in the wave guide. To quantify this effect the higher harmonic modes are used to determine the relative acoustical nonlinearity parameter β'. Previous studies show that this procedure offers a good possibility to detect micro-structural damages like plastic deformation [1] and fatigue damage [2] in metal as well as thermal fatigue [3] and impact damages [4] in composites. Furthermore [3] and [4] show that this procedure is much more sensitive due to microstructural damages than linear wave propagation properties like the group velocity.

To analyze the damage state of a plate like structure Lamb waves are used because they can travel long distances by covering the whole thickness. Furthermore they can be launched and detected easily by piezoelectric actuators and sensors, respectively. [5]

In this paper the impact of fatigue damage in unidirectional composite due to cyclic tensile load on the relative acoustical nonlinearity parameter β', as defined in [2, 3], is investigated. Furthermore, the damage state will be visualized by an ultrasonic imagine method.

Because of the multi-modal and dispersive nature of Lamb waves the extraction of amplitudes with a certain frequency implicates some difficulties. Therefore, the separation of modes due to the different corresponding group velocities is used to determine the required modes at first. Afterwards the magnitude of the amplitudes is extracted with the wavelet transform. The Lamb waves are launched and detected by a piezoelectric actuator and sensor, respectively.

Copyright © Inria (2014)

2. LAMB WAVE PROPAGATION IN THIN PLATES

2.1 Lamb waves

The phenomenon of elastic waves in thin plates was first documented by Horace Lamb in 1917 [6]. Starting with the three fundamental equations of the continuum mechanics, the stress-strain relation, the balance of momentum and the Green's deformation tensor for isotropic material and using the index notation the equation of motion can be obtained as

$$(\lambda+\mu)u_{j,ji}+\mu u_{i,jj}+\rho b_i=\rho\ddot{u}_i. \tag{1}$$

λ and μ are the Lamé-coefficients, ρ is the density, u_i the displacement vector and b_i force per unit mass. Solving (1) considering the boundary conditions of stress-free surfaces the Rayleigh-Lamb equation can be found

$$\frac{\tan qh/2}{\tan ph/2}=-\left(\frac{4k^2pq}{(q^2-k^2)^2}\right)^{\pm 1}. \tag{2}$$

The exponent ± 1 indicates the symmetric and antisymmetric mode. h is the plate thickness, k the wave number and p and q are defined as

$$p=\sqrt{k_l^2-k^2}\quad\text{and}\quad q=\sqrt{k_t^2-k^2}, \tag{3}$$

respectively. k_l and k_t are the wave numbers of the longitudinal and transversal wave. Therefore, (2) describes the propagation of Lamb waves in an isotropic media. Due to the more complex stiffness matrix for transversal-isotropic media it follows for the boundary condition for Lamb-wave propagation in a lamina [7]

$$\begin{bmatrix}\sigma_{(z=z_u)}\\ \sigma_{(z=z_o)}\end{bmatrix}=\begin{bmatrix}\mathbf{D}^- & \mathbf{D}^+\mathbf{H}\\ \mathbf{D}^-\mathbf{H} & \mathbf{D}^+\end{bmatrix}\begin{bmatrix}\mathbf{a}^+\\ \mathbf{a}^-\end{bmatrix}=0. \tag{4}$$

The subscript $\pm$ indicates the upper and lower boundary of the transversal-isotropic layer, $\sigma=[\sigma_{13}\ \sigma_{23}\ \sigma_{33}]^T$, $\mathbf{a}$ is the amplitude vector, $\mathbf{D}=[\mathbf{d}_1\ \mathbf{d}_2\ \mathbf{d}_3]$ and $\mathbf{H}=diag(e^{ik_{z_1}h}\ e^{ik_{z_2}h}\ e^{ik_{z_3}h})$. $\mathbf{d}_j$ is related to the wave number k_{z_j}, an eigenvalue of the Christoffel equation given by [8]

$$(C_{ijkl}k_jk_n-\rho\omega^2\delta_{il})m_l=0 \tag{5}$$

and is defined as $\mathbf{d}_j=C_{i3kl}n_l\mathbf{m}_j$ $(i,j,k,l=1,2,3)$. C_{i3kl} is the stiffness matrix of the transversal-isotropic layer, n_l is the direction cosine of the wave propagation and $\mathbf{m_j}$ is the polarization vector, the eigenvector to the eigenvalue k_{z_j}. In (5) ω is the angular frequency and δ_{ij} the Kronecker delta.

2.2 Higher-harmonic Lamb waves

In a nonlinear medium due to material imperfections, monofrequency excitation causes a structural response not only at the excitation frequency but also at higher harmonic frequencies, that are a multiple of the primary excited frequency. Figure 1 shows the differences of wave propagation in linear (ideal) and nonlinear (imperfect) media. Those higher harmonics usually have a very small amplitude and hence subside very quickly. To overcome this problem and to detect even higher harmonics accurately a cumulative effect is used. If certain conditions are satisfied the amplitude of a specific higher harmonic mode grows with propagation distance. This ensures a better signal-to-noise ratio and therefore, a more accurate detection.

These conditions have been analyzed by Deng et al. in detail in the last couple of years [9–12]. It was found that three conditions need to be satisfied to generate so called cumulative higher harmonics.

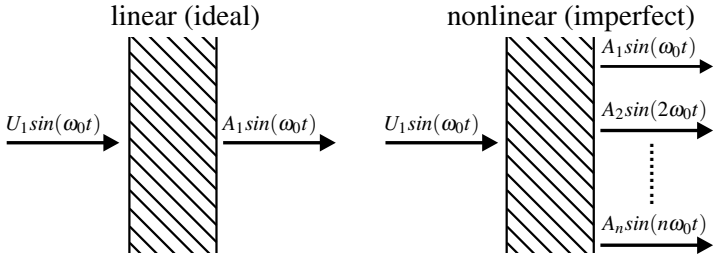
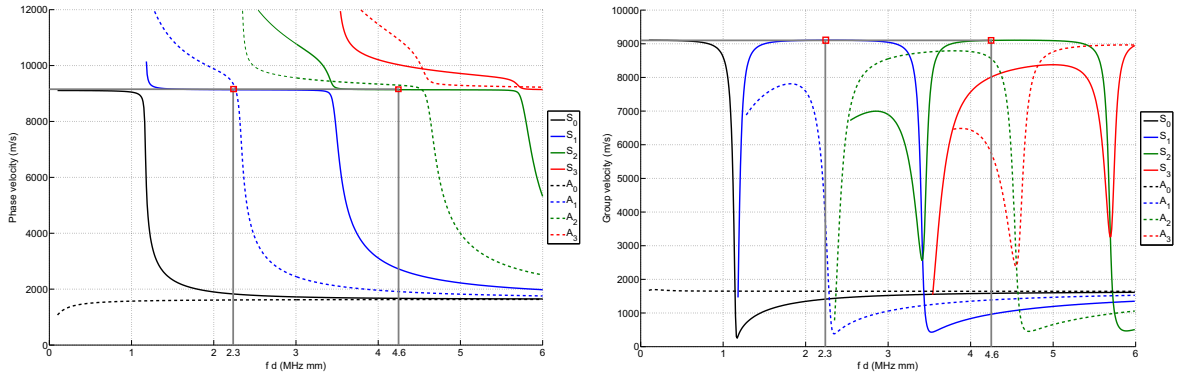


Figure 1 : Wave propagation in a linear and nonlinear medium



(a) Dispersion curves of the phase velocity

(b) Dispersion curves of the group velocity

Figure 2 : Dispersion curves of a carbonfiber / epoxy $[0]_4$ composite for wave propagation in fiber direction

The first condition for a cumulative effect is the phase velocity matching of the primary excited and higher harmonic wave at ω and $n\omega$, respectively. Beside the phase velocity matching the group velocity of the primary and higher harmonic wave at ω and $n\omega$ has to be equal as a second condition. Finally a power flux form the primary excited to the higher harmonic mode is required. [13, 14] show that this condition is only satisfied for symmetric Lamb wave modes. Furthermore, the power flux is zero for the S_0-mode [10]. Considering these conditions in this study the second harmonic Lamb wave generation is used as a nonlinear wave propagation technique to analyze the damage state. As done before in [3, 4] for composite plate-like structures the S_1-S_2 mode pair is applied.

To find the frequencies ω and 2ω corresponding to the Lamb wave modes S_1 and S_2 the non-trivial solutions of (4) are determined numerically. The results give the dispersion curves plotted in figure 2. Figure 2(a) shows the dispersion curves of the phase velocity and figure 2(b) of the group velocity. In addition the matching phase and group velocities for the primary excited S_1 at the frequency ω and second harmonic S_2 mode at 2ω are marked. The stiffness coefficients and density of the used material are given in table 1.

Table 1 : Stiffness coefficients and density of the unidirectional composite

C_{11} (GPa)	C_{12} (GPa)	C_{22} (GPa)	C_{23} (GPa)	C_{44} (GPa)	C_{66} (GPa)	ρ (kg m^{-3})
122.3	8.08	2.38	5.82	3.75	4	1.47

2.3 Relative acoustical nonlinearity parameter

As given in [3] for Lamb waves the acoustical nonlinearity parameter β is defined as

$$\beta = \frac{8}{k^2 X} \frac{A_2}{A_1^2} f, \tag{6}$$

where X is the propagation distance, A_2 and A_1 are the amplitudes of the second harmonic and primary mode, respectively, and f is the feature function. As said before the non-zero power flux condition of cumulative second harmonic modes is not satisfied for antisymmetric Lamb wave modes and therefore, the S_1-S_2 mode pair will be analyzed. In this case the feature function of the Lamb wave nonlinearity parameter can be written as

$$f = \frac{\cosh^2(p'h)}{\cosh(2p'h)} \left(1 - \frac{k^2 + q'^2}{2k^2}\right). \tag{7}$$

Here, p' and q' are defined as

$$p' = \sqrt{k^2 - k_l^2} \text{ and } q' = \sqrt{k^2 - k_t^2}, \tag{8}$$

respectively, [3]. Considering this the feature function depends on the frequency, the wave number and the thickness of the specimens. For the experimental investigation of fatigue damages in this research only one wave pair at a constant frequency is used and all specimens have the same dimensions. In this case the feature function is constant and might be neglected as done in [3]. Furthermore, the acoustical nonlinearity parameter depends on the propagation distance which is constant in this research as well. Because of this just the proportionality of the amplitudes' ratio can be used. It is defined as the relative acoustical nonlinearity parameter β'

$$\beta' = \frac{A_2}{A_1^2} \propto \beta. \tag{9}$$

3. Experimental Procedure

3.1 Specimens

The fatigue damage is analyzed in unidirectional composite specimens with different damage states. The specimens consist of carbon fibres in an epoxy matrix with a stacking sequence $[0]_4$ and have the dimensions 600 mm times 80 mm times 2.3 mm. The degradation is realized by a cyclic pulsating load. The upper limit of each cycle is 200 kN and the lower limit 10 kN. To generate specimens with different damage states, the specimens vary in the number of cycles they are exposed. In total nine specimens are investigated. One is a reference specimen and therefore, is left undamaged. The rest are damaged by cyclic tensile load whereby for each number of cycles two specimens are prepared. This ensures to analyze if a certain number of cycles leads to a similar damage state in different specimens. Table 2 gives the number of cycles and the corresponding amount of specimens.

Table 2 : Damage state of Specimens

Number of cycles	Number of specimens
0	1
5000	2
10000	2
15000	2
20000	2

3.2 Experimental investigation of the nonlinear wave propagation

3.2.1 Experimental set-up and procedure

Figure 3 provides a schematic of the experimental set-up for the investigation of the nonlinear wave propagation. The specimens have a thickness of 2.3 mm. Relating to this Lamb waves are generated with a center frequency of 1 MHz by a function generator and launched by a piezoelectric actuator via an amplifier. A tone burst signal of 2 sine cycles is used for the excitation of the required primary excited Lamb wave mode. The total amplitude is 50 V_{pp}. The primary excited and second harmonic wave modes are detected simultaneously by a 16-bit transient recorder via a piezoelectric sensor. The time-domain signal is measured with a sampling rate of 105 MHz and averaged 1000 times by the transient recorder to improve the signal-to-noise ratio. All measurements are taken with a propagation distance of 20 cm to minimize near-field-effects. Each measurement is repeated 10 times to improve the statistical accuracy. The piezoelectric actuator and sensor are fixed to the specimens permanently.

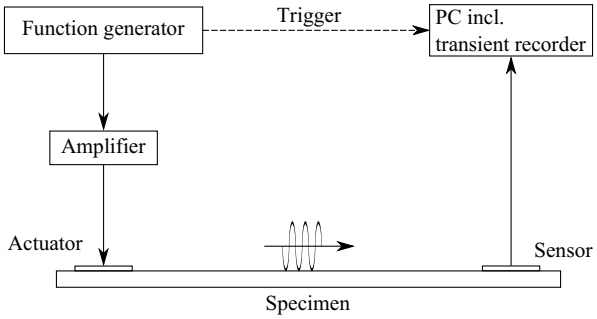
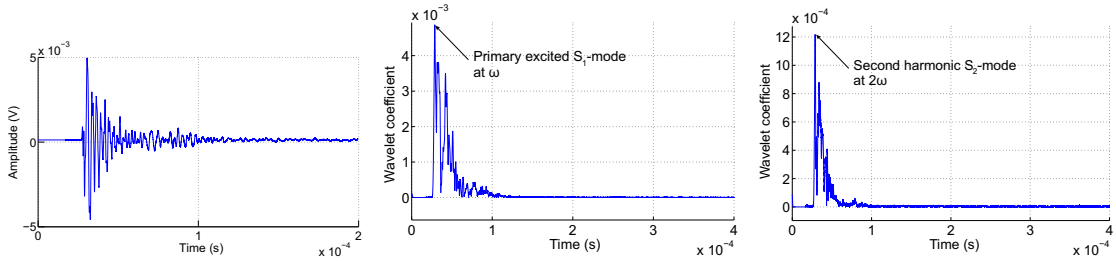


Figure 3 : Block diagram of the experimental setup.

3.2.2 Signal processing

Because of the multi-modal and dispersive nature of Lamb waves a time-frequency method is necessary to extract the amplitudes of the primary excited and second harmonic mode accurately. As shown in [15] the wavelet transform with the Morlet wavelet as mother wavelet is a suitable tool. Furthermore the Morlet wavelet has in contrast to the Gabor wavelet, that might be used as well, a better frequency solution. The worse time resolution is not significant for the amplitude extraction.

Using the wavelet transform a wave mode at a frequency ω with the group velocity c_g is represented by a wavelet coefficient magnitude peak corresponding to the frequency ω. Because of the multi-modal nature of Lamb waves a wavelet coefficient magnitude peak corresponding to the primary excited frequency can be related to several modes. As shown in figure 2(a) an excitation at a frequency of 2.3 MHz mm generates not only the required S_1-mode but also the S_0-, A_0- and



(a) A typical time signal of the S_1-S_2 mode pair

(b) Signal after Wavelet transform to extract the wavelet coefficients corresponding to the amplitudes of the S_1-mode at the primarily excited frequency

(c) Signal after Wavelet transform to extract the wavelet coefficients corresponding to the amplitudes of the S_2-mode at the second harmonic frequency

Figure 4 : Signal processing

A_1-mode. Considering figure 2(b) these modes travel along the the specimen with different group velocities. Comparing the group velocities of the not required S_0-, A_0- and A_1-modes with the S_1-mode shows that the essential S_1-mode has the highest group velocity and therefore, arrives first at the piezoelectric sensor. Consequently the first magnitude peak represents the amplitude of the S_1-mode. The wavelet coefficient peak corresponding to the second harmonic frequency is clearly assigned to the second harmonic S_2-mode, because there are no other modes at this frequency. This ensures the accurate extraction of the two required Lamb wave amplitudes despite the multi-modal and dispersive nature of Lamb waves.

Figure 4(a) shows a typical time domain signal of the S_1-S_2-mode pair captured by the piezoelectric sensor after a propagation distance of 20 cm. Figure 4(b) and 4(c) present the wavelet coefficient corresponding to the primary and the second harmonic frequency, respectively. The magnitude peaks corresponding to the S_1- and second harmonic S_2-mode are marked.

3.3 Determination of the damage state - visualization of the damage caused by cyclic tensile load

To analyze the damage state of the specimens two specimens are analyzed by a ultrasonic method to visualize defects. This is done for the undamaged and apparently most damaged specimen based on the results of the wave propagation.

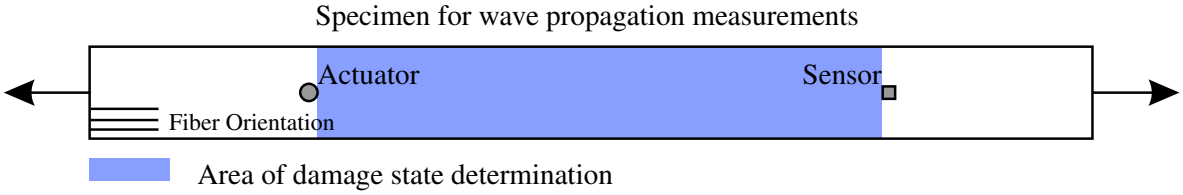
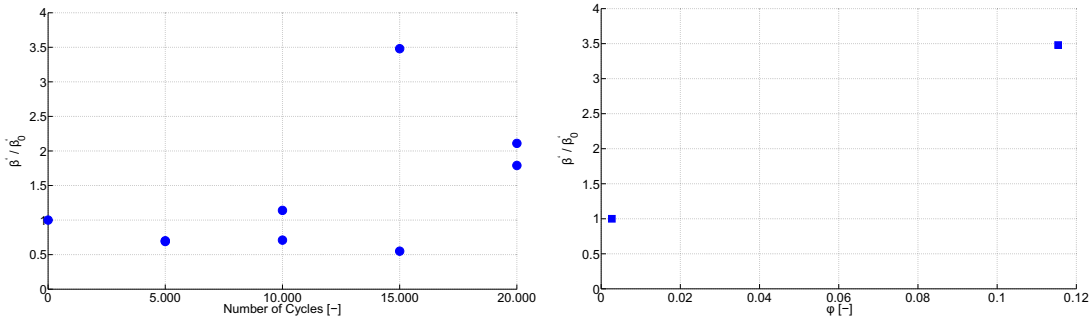


Figure 5 : Part of the damaged specimens to obtain the material properties.

This procedure allows to visualize initial damages like delaminations, porosities and entrapped air caused by the manufacturing and damages caused by the cyclic tensile load. The result of the ultrasonic measurement is a C-scan, in that the different amplitudes at the receiver are indicated by colors. Considering the back wall echo damages correspond to regions of lower amplitudes. These areas are extracted and related to the complete scanning area to obtain the damage state parameter φ.

4. RESULTS

Figure 6 shows the results of the nonlinear wave propagation analysis (figure 6(a)) and the visualisation of the damage state by an ultrasonic imaging method (figure 6(b)).



(a) β'/β_0' against the number of cycles (b) β'/β_0' against φ

Figure 6 : Results of the normalized relative acoustical nonlinearity parameter β'/β_0' and the damage state φ

5. CONCLUSION

Figure 6(a) shows a variation of the normalized, relative acoustical nonlinearity for the different specimens. This indicates different damage states of the specimens, because the second harmonic generation depends on the number of defects in the waveguide. The visualisation of the damage state of the reference and a damaged specimen supports this. In figure 6(b) it is clearly shown that the damage state φ of the damaged specimen is much higher than of the undamaged reference specimen.

Furthermore the reference specimen is more damaged than some specimens that were introduced to cyclic tensile load which might be related to initial manufacturing defects at the reference specimen and comparing the results of the specimens with different number of cycles indicates, the same cyclic load does not lead to the same damage state. This is caused by a complex damaging procedure due to the cyclic tensile load due to the structure of a unidirectional composite layer.

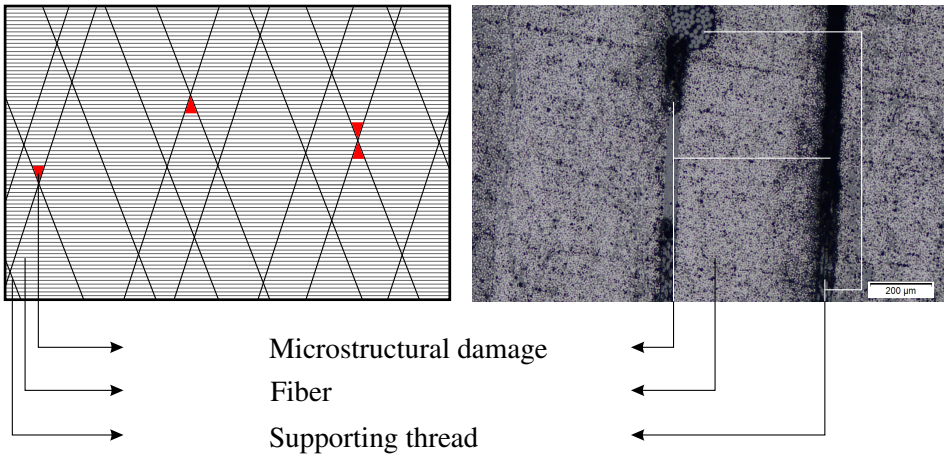


Figure 7 : Schematic layout and a micrograph of a unidirectional CFK prepreg with microstructural damages due to tensile load

Considering the manufacturing process the specimens are part of a plate that is made out of four prepreg layers. These layers were placed by a tape laying machine and cooked under high pressure. Due to regions of low pressure pores can occur. To avoid a displacement of the fibers while setting they

are fixed by threads across the prepreg. Introducing high tensile load to the specimens these threads break first. Especially at crossing point of two threads these lead to microstructural damages. Due to the cyclic tensile load these damages grow. Because the initial damage due to cracking of the threads is not reproducible the initial damage state is different for each specimen. Figure 7 shows the structure of a unidirectional prepreg and the locations of initial damages due to threads cracking schematically on the left hand side and by a microscope image on the right hand side.

6. OUTLOOK

The effect of the cyclic tensile load on the unidirectional composite specimens will be analyzed more in detail. Therefor considering all specimens the material parameter will be experimentally obtained and the visualisation of the damage state by an imaging method will be done. Based on the results the correlations between the normalized, relative acoustical nonlinearity parameter, the material properties and the damage state to each other will be investigated.

ACKNOWLEDGEMENT

The imaging ultrasonic test, done by Ingenieurbüro Dr. Hillger - Ultrasonic-Techniques, are gratefully acknowledged.

REFERENCES

[1] C. Pruell, J.-Y. Kim, J. Qu, and L. J. Jacobs. Evaluation of plasticity driven material damage using lamb waves. *Applied Physics Letters*, 91(23):231911, 2007.

[2] C. Pruell, J.-Y. Kim, J. Qu, and L. J. Jacobs. Evaluation of fatigue damage using nonlinear guided waves. *Smart Materials and Structures*, 18(3):035003, 2009.

[3] W. Li, Y. Cho, and J. D. Achenbach. Detection of thermal fatigue in composites by second harmonic lamb waves. *Smart Materials and Structures*, 21(8):085019, 2012.

[4] N. Rauter, R. Lammering. Experimental investigation of impact damages in composites by second harmonic lamb waves. In *Proceedings of the 6th ECCOMAS Thematic Conference on Smart Structures and Materials*, 2013.

[5] Victor Giurgiutiu. *Structural Health Monitoring: with Piezoelectric Wafer Active Sensors*. Elsevier/Academic Press, Burlington and MA, 2008.

[6] H. Lamb. On waves in an elastic plate. *Proceedings of the Royal Society A: Mathematical, Physical and Engineering Sciences*, 93(648):114–128, 1917.

[7] L. Wang and S. I. Rokhlin. Stable reformulation of transfer matrix method for wave propagation in layered anisotropic media. *Ultrasonics*, 39(6):413–424, 2001.

[8] J. L. Rose. *Ultrasonic waves in solid media*. Cambridge University Press, Cambridge and New York, 1999.

[9] M. Deng. Cumulative second-harmonic generation of lamb-mode propagation in a solid plate. *Journal of Applied Physics*, 85(6):3051, 1999.

[10] M. Deng. Analysis of second-harmonic generation of lamb modes using a modal analysis approach. *Journal of Applied Physics*, 94(6):4152, 2003.

[11] M. Deng, P. Wang, and X. Lv. Experimental verification of cumulative growth effect of second harmonics of lamb wave propagation in an elastic plate. *Applied Physics Letters*, 86(12):124104, 2005.

[12] M. Deng and J. Pei. Assessment of accumulated fatigue damage in solid plates using nonlinear lamb wave approach. *Applied Physics Letters*, 90(12):121902, 2007.

[13] Y. Liu, J.-Y. Kim, L. J. Jacobs, J. Qu, and Z. Li. Experimental investigation of symmetry properties of second harmonic lamb waves. *Journal of Applied Physics*, 111(5):053511, 2012.

[14] Y. Liu, J. Y Kim, L. J. Jacobs, and Z. Li. Modal preference of cumulative second harmonic generation in lamb waves. In *Review of Progess in Quantitative Nondestructive Evaluation: Volume 31*, volume 1430 of *AIP Conference Proceedings*, pages 277–283. AIP, 2012.

[15] J. Lin and L. Qu. Feature extraction based on morlet wavelet and its application for mechanical fault diagnosis. *Journal of Sound and Vibration*, 234(1):135–148, 2000.